Ecology and Evolution

Open Access

Saturating light and not increased carbon dioxide under ocean acidification drives photosynthesis and growth in *Ulva rigida* (Chlorophyta)

Ralf Rautenberger[1,*], Pamela A. Fernández[1], Martina Strittmatter[2], Svenja Heesch[3], Christopher E. Cornwall[1,4], Catriona L. Hurd[1,4] & Michael Y. Roleda[1,5,*]

[1]Department of Botany, University of Otago, P.O. Box 56, Dunedin 9054, New Zealand
[2]The Scottish Association for Marine Science, Scottish Marine Institute, Oban, Argyll, PA37 1QA, Scotland
[3]Irish Seaweed Research Group, Ryan Institute for Environmental, Marine and Energy Research, National University of Ireland, Galway (NUIG), University Road, Galway, Ireland
[4]Institute for Marine and Antarctic Studies, University of Tasmania, Hobart, Tasmania 7001, Australia
[5]Bioforsk Norwegian Institute for Agricultural and Environmental Research, Kudalsveien 6, 8049 Bodø, Norway

Keywords
Bicarbonate, C:N ratio, carbon physiology, carbon-concentrating mechanism, carbonic anhydrase, chlorophyll fluorescence, F_v/F_m, pigments, seaweed, stable carbon isotope.

Correspondence
Michael Y. Roleda, Bioforsk Norwegian Institute for Agricultural and Environmental Research, Kudalsveien 6, 8049 Bodø, Norway
Tel: +47 406 04 100;
E-mail: Michael.Roleda@bioforsk.no

Present address
Ralf Rautenberger, Instituto de Ciencias Marinas y Limnológicas, Universidad Austral de Chile, Casilla 567, Valdivia, Chile

Funding Information
This work was funded by the Royal Society of New Zealand Marsden Fund (Grant UOO0914) and the German Research Foundation (DFG: RA 2030/1-1).

Received: 8 October 2014; Revised: 10 December 2014; Accepted: 12 December 2014

Ecology and Evolution **2015; 5(4): 874–888**

doi: 10.1002/ece3.1382

*Authors have equal contributions.

Abstract

Carbon physiology of a genetically identified *Ulva rigida* was investigated under different $CO_{2(aq)}$ and light levels. The study was designed to answer whether (1) light or exogenous inorganic carbon (Ci) pool is driving growth; and (2) elevated $CO_{2(aq)}$ concentration under ocean acidification (OA) will downregulate CA_{ext}-mediated HCO_3^- dehydration and alter the stable carbon isotope ($\delta^{13}C$) signatures toward more CO_2 use to support higher growth rate. At pH_T 9.0 where $CO_{2(aq)}$ is <1 μmol L^{-1}, inhibition of the known HCO_3^- use mechanisms, that is, direct HCO_3^- uptake through the AE port and CA_{ext}-mediated HCO_3^- dehydration decreased net photosynthesis (NPS) by only 56–83%, leaving the carbon uptake mechanism for the remaining 17–44% of the NPS unaccounted. An in silico search for carbon-concentrating mechanism elements in expressed sequence tag libraries of *Ulva* found putative light-dependent HCO_3^- transporters to which the remaining NPS can be attributed. The shift in $\delta^{13}C$ signatures from –22‰ toward –10‰ under saturating light but not under elevated $CO_{2(aq)}$ suggest preference and substantial HCO_3^- use to support photosynthesis and growth. *U. rigida* is Ci saturated, and growth was primarily controlled by light. Therefore, increased levels of $CO_{2(aq)}$ predicted for the future will not, in isolation, stimulate *Ulva* blooms.

Introduction

The world's oceans are a sink for CO_2 that has been released through anthropogenic processes since the industrial revolution (~1850). This process buffers climate change in the terrestrial system, but perturbs the seawater carbonate system, and is reducing the pH of the surface ocean, termed ocean acidification (OA) (Takahashi et al.

2014). In the next century, atmospheric CO_2 concentrations are projected to increase from 395.93 ppm (October 2014; www.CO2now.org) to a maximum of 1142 ppm in 2100 (IPCC 2013): the 192% increase will consequently reduce global surface ocean pH by 0.4 units (Meehl et al. 2007). OA may have a profound impact on organismal carbon physiology, trophic dynamics, biogeochemical cycles, and ecosystem functions and services (Gattuso and Hansson 2011; Roleda and Hurd 2012; Koch et al. 2013).

Seaweeds are macroscopic, multicellular marine algae. They are foundation species and provide energy to higher trophic levels. They belong to three distinct evolutionary groups: green (Chlorophyta), brown (Ochrophyta), and red (Rhodophyta) seaweeds. Most seaweeds are able to take up both CO_2 and HCO_3^- from the surrounding seawater as inorganic carbon (Ci) sources for photosynthesis. CO_2 can enter seaweed cells through the plasma membranes by passive diffusion. However, this process is very slow in water and dissolved carbon dioxide ($CO_{2(aq)}$) makes up less than 1% of the total Ci. On the other hand, HCO_3^- is the most abundant ionic form of Ci (92%) but requires specific carriers for transport across membranes (Björk et al. 1992; Sharkia et al. 1994).

To overcome the low availability of $CO_{2(aq)}$ to supply the ribulose-1,5-bisphosphate carboxylase/oxygenase (RuBisCO) for photosynthetic carbon fixation, most seaweeds have developed strategies of utilizing HCO_3^-. These strategies include as follows: (1) extracellular carbonic anhydrase (CA_{ext})-mediated HCO_3^- dehydration and subsequent passive diffusion of CO_2 into the cell (Björk et al. 1992). (2) Direct HCO_3^- uptake by the anion-exchange protein AE1, similar to that present in mammalian red blood cells (Drechsler and Beer 1991; Drechsler et al. 1993; Sharkia et al. 1994). The internal inorganic carbon (Ci) pool is stored primarily as HCO_3^-; consequently, this requires intracellular carbonic anhydrase (CA_{int})-mediated HCO_3^- dehydration to supply CO_2 to RuBisCO for photosynthetic carbon fixation (Fernández et al. 2014). For the seaweed genus *Ulva*, that is the focus of this study, the relative contribution of CA_{ext}-mediated HCO_3^- utilization versus direct HCO_3^- uptake to supply CO_2 for photosynthesis varies substantially among different species where species are identified based on traditional taxonomic classification (Larsson and Axelsson 1999). (3) An indirect HCO_3^- use operates in conjunction with metabolically mediated proton (H^+) flux where H^+ extrusion creates a local acidified zone within the diffusion boundary layer at the seaweed surface, thereby stimulating a pH-dependent conversion of HCO_3^- to CO_2 (Björk et al. 1992; Beer et al. 2008). Such uncatalyzed or spontaneous dehydration of HCO_3^- can, however, be slow and may be insufficient to support high photosynthetic and growth rates (Cook et al. 1986).

Ulva is a globally ubiquitous seaweed, well known for causing massive macroalgal blooms that can have negative environmental and economic impacts (McGlathery 2001; Sun et al. 2008; Pang et al. 2010). The drivers of *Ulva* primary production and growth are variously attributed to light (Aldridge and Trimmer 2009), inorganic nutrients (Coutinho and Zingmark 1993), CO_2 (Xu and Gao 2012), and their interactions. Under a saturating light (200–500 μmol photons m^{-2} s^{-1}) growth of *Ulva curvata* can become limited by the supply of inorganic nitrogen (Coutinho and Zingmark 1993). When grown under a subsaturating light (100 μmol photons m^{-2} s^{-1}) (but unspecified nutrient concentration), the growth of *Ulva prolifera* cultivated from spores was reported to increase by ~20% d^{-1} when CO_2 was increased by 156% (Xu and Gao 2012). Whether or not a saturating light will further enhance the growth of *Ulva* under elevated CO_2 is unknown.

There are many studies showing that HCO_3^- is the primary source of Ci for *Ulva* species (Drechsler and Beer 1991; Björk et al. 1992, 1993; Drechsler et al. 1993; Sharkia et al. 1994). Therefore, it is unlikely that the predicted increase in $CO_{2(aq)}$ due to OA will have an effect on the rates of photosynthesis and growth in *Ulva* (e.g. Xu and Gao 2012). Nevertheless, researchers continue to pursue this line of research (e.g. Pajusalu et al. 2013; Olischläger et al. 2013), suggesting that increased levels of $CO_{2(aq)}$ will cause increased growth rate in *Ulva*. Here, we demonstrate that light, and not Ci, is the main driver for growth of *Ulva* and suggest that increased levels of $CO_{2(aq)}$ predicted for the future will not, in isolation, stimulate photosynthesis and growth of *Ulva*.

This study is important and timely because it questions the validity of the current dogma that increasing CO_2 will promote (harmful) algal blooms and drive ecosystem "winners and losers". There is currently a very limited understanding of algal carbon physiology on an organismal level (e.g. Kübler et al. 1999) and on the environmental drivers of basic physiological mechanisms (e.g. Raven 1991) such as photosynthesis and growth. Moreover, the combined physiological and molecular approaches to investigate key driver for *Ulva* growth confers novelty in this work.

The photosynthetic carbon physiology and growth of a genetically identified *Ulva* species under different $CO_{2(aq)}$ and light levels were investigated. We hypothesized that (1) under current concentration of $CO_{2(aq)}$, exogenous Ci is saturating for photosynthesis and growth of *Ulva rigida*; (2) *U. rigida* has several putative HCO_3^- use mechanisms other than the known inhibitor-sensitive CA_{ext}-catalyzed dehydration of HCO_3^- and direct uptake of HCO_3^- through the anion-exchange (AE) port; and (3) elevated concentrations of $CO_{2(aq)}$ predicted for the

future will not affect *U. rigida* growth. The experiment was designed to answer whether (1) light or exogenous Ci pool is limiting *U. rigida* growth; (2) elevated Ci (CO_2 and HCO_3^-) under OA will support a higher growth rate; (3) CA_{ext}-mediated HCO_3^- dehydration is downregulated when *Ulva* is grown under a high $CO_{2(aq)}$ concentration; and (4) the hypothetical shift to more CO_2 use under OA will alter the stable carbon isotope ($\delta^{13}C$) signature (*cf* Maberly et al. 1992; Raven et al. 2002; Giordano et al. 2005) and the higher available Ci under OA relative to constant nutrient supply will increase the molar carbon to nitrogen (C:N) ratio (*cf* van de Waal et al. 2010).

Materials and Methods

Algal material and stock culture conditions

Sheet-forming *Ulva* thalli (Fig. 1) were collected on 5 October 2011 from the subtidal at the entrance (3 m depth) of Otago Harbour, southern New Zealand (Aramoana, 45.8°S, 170.7°E) and transported in a cooled container to the laboratory. Several algal discs (Fig. 1 inset) were excised from one individual and cultivated in 5-L glass vessels with nutrient-enriched seawater, formulated using the ESNW recipe (Harrison et al. 1980; Berges et al. 2001), which was used throughout the experiment. To avoid significant pH drop, the ESNW was prepared with one-third of the full strength concentrations of phosphate, iron-EDTA (pH <6.0), trace metals II (pH <6.0) and vitamins stock solutions and 5 μmol L^{-1} of $NaNO_3$-N; the final seawater pH was pH_T 7.97, ~0.08 pH unit lower than ambient seawater. The *Ulva* clones were grown under photosynthetic photon fluence rate (PPFR) of 50 μmol photons m^{-2} s^{-1} over the waveband 400–700 nm (Philips TLD 18W/840 Cool White; Philips, Amsterdam, The Netherlands) and 12 h: 12 h, light:dark cycle at 13°C in a Phytotron Climate Simulator cabinet (Contherm Scientific Ltd, Lower Hutt, New Zealand). Clones were grown below the saturating irradiance of 79 ± 9 μmol photons m^{-2} s^{-1} (R. Rautenberger, unpubl. data) to avoid rapid growth, nutrient depletion, and swarmer release. After 8 months clonal propagation, algal discs (3 cm^2, 25 mg FW) were used in the experiments below.

Figure 1. Sheet-forming *Ulva* from the subtidal flat at the entrance of Otago Harbour, southern New Zealand. Inset: discs of genetically identified *Ulva rigida* clones used in the experiment.

Two specimens grown from the clonal cultures were prepared as herbarium vouchers and deposited in the herbarium of the University of Otago (OTA; Thiers 2014) under the accession numbers OTA63969 and OTA63970. Material of the latter specimen was prepared for genetic identification by excising a disc from the freshly harvested thallus and drying it in silica gel.

Genetic identification and life history of the cultured strain

The *Ulva* strain (SBDN 247) was genetically identified using the methods in Heesch et al. (2009), except for the following differences: DNA was extracted and PCR products were purified using commercial kits (NucleoSpin® Plant II, Macherey-Nagel, Düren, Germany, and PureLink® PCR Purification Kit, Invitrogen, Germany, respectively). Sequence alignments of the large subunit of the plastid-encoded RuBisCO gene region (*rbc*L) were analyzed under the maximum-likelihood (ML) criterion using the default settings in RAxML v.7.2.2 (Stamatakis 2006). Our *rbc*L sequence (European Nucleotide Archive [ENA] accession no. LK022428) was found to be 100% identical to *rbc*L sequences from *U. rigida* samples collected in New Zealand (e.g. GenBank accession number EF110302; Heesch et al. 2009), Europe (EU484408; Loughnane et al. 2008) and Chile (AY422564: Hayden and Waaland 2004). The phylogenetic analysis placed our strain in a well-supported clade with the above sequences (data not shown), confirming its identification as *Ulva rigida* C.Agardh.

Swarmers released from clonal tissue were positively phototactic indicating that the cultivated strain was a gametophyte, that is, the haploid generation (Guiry and Guiry 2014). Cultivation of the released gametes failed to develop parthenogenetically, suggesting that swarmers were most likely male gametes, which, in contrast to female swarmers, have lower capacity to germinate without fertilization (Koeman and van den Hoek 1981).

Carbon physiology: inhibition of known bicarbonate-use mechanisms

Acetazolamide (AZ, CAS number 59-66-5) and 4,4′-diisothiocyanatostilbene-2,2′-disulfonate (DIDS, CAS

number 207233-90-7) are inhibitors with high specificity for blocking the catalyzed external dehydration of HCO_3^- and the direct HCO_3^- uptake through the anion-exchange (AE) port, respectively (Björk et al. 1992; Axelsson et al. 1995, 1999; Axelsson et al. 2000; Herfort et al. 2002; Suffrian et al. 2011). Both mechanisms operate independently: the addition of these inhibitors in the absence of other HCO_3^- uptake mechanisms can result in an almost complete inhibition of net photosynthesis (Axelsson et al. 1995; Larsson and Axelsson 1999; Fernández et al. 2014). A concentration of 300 μmol L^{-1} DIDS to inhibit the direct HCO_3^- uptake and 100 μmol L^{-1} AZ to inhibit CA_{ext} were selected based on the dose response curves of Herfort et al. (2002), and the standard utilization of these concentrations across studies on the Ci-use mechanisms of micro- and macroalgal species (e.g. Björk et al. 1992; Axelsson et al. 1995, 1999; 2000; Young et al. 2001; Herfort et al. 2002; Suffrian et al. 2011; van Hille et al. 2014). The 10 mmol L^{-1} stock solution of AZ (≥99%, Sigma-Aldrich, St. Louis, MO, USA) was prepared by dissolving the powder in a basic medium (10 mmol L^{-1} NaOH in MilliQ, 18.3 MΩ cm) while the 30 mmol L^{-1} stock solution of DIDS (≥80% elemental analysis, Sigma-Aldrich) was prepared by dissolving the powder in MilliQ. The stock solutions were freshly prepared and kept at 4°C and dark.

Algal discs were acclimated for 2 days under pH_T 9.0 where Ci is mainly available as HCO_3^- (700 μmol L^{-1}) with minimal $CO_{2(aq)}$ (<1 μmol L^{-1}). Seawater was adjusted using equal amounts of 0.2 mol L^{-1} NaOH and 0.2 mol L^{-1} $NaHCO_3$ (Roleda et al. 2012a). After 2 days, inhibition of photosynthetic O_2 evolution (n = 3) under the same pH_T = 9.0 was measured inside a 154-mL transparent acrylic glass chamber equipped with an optode, that is, FOXY–R fiber optic oxygen sensor coupled to the USB–2000 spectrophotometer (Ocean Optics, Dunedin, FL, USA) and the PC interface. The seawater was continuously stirred (650 rpm) to create a homogenous O_2 profile. To avoid photorespiration due to high O_2 concentrations and temperature, the seawater was initially adjusted to 100 ± 20 μmol O_2 L^{-1} using N_2 gas and kept constant at 12 ± 1°C, respectively. Net oxygen evolution of individual *U. rigida* discs was recorded (OOISensor 1.0 software; Ocean Optics Inc., FL, USA) at a PPFR of 250 μmol photons m^{-2} s^{-1} (400–700 nm). Oxygen concentration inside the chamber was recorded for 20 min before the inhibitors were added and then for a further 2 × 15 min following the sequential addition of the two inhibitors (e.g. DIDS-AZ and AZ-DIDS; n = 3). The oxygen concentration was measured continuously for a total of 50 min per sample. The rate of oxygen evolution was calculated using a linear regression for every stepwise incubation period, that is, the whole incubation time (20 min) before application of the inhibitors, and after every application of each inhibitor (2 × 15 min). The oxygen concentration (μmol O_2 L^{-1}) was measured after Millero and Poisson (1981) and García and Gordon (1992), and corresponding % inhibition of net photosynthetic (NPS) rate was calculated.

In silico detection of carbon-concentrating mechanisms elements in expressed sequence tag libraries of *Ulva*

To test our hypothesis on *Ulva* having different Ci uptake mechanisms other than the known inhibitor-sensitive CA_{ext}-catalyzed dehydration of HCO_3^- and direct uptake of HCO_3^- through the AE port, we searched one expressed sequence tag (EST) library of *U. prolifera* (Jia et al. 2011) publicly available in the dbEST database (Boguski et al. 1993) for putative carbon-concentrating mechanism (CCM) elements. A number of described CCM proteins of the unicellular green alga *Chlamydomonas reinhardtii* were used in a tblastn search against the *U. prolifera* EST data set and included the following protein sequences: alpha carbonic anhydrases (CAH1 [accession number BAA14232], CAH3 [EDP00852.1]), beta carbonic anhydrases (CAH6 [AAR82947.1], CAH8 [ABS87675.1]), gamma carbonic anhydrase (CAG2 [XP_001701594]), nuclear transcriptional regulators of CCM elements (CIA5 [AAG37909.1], LCR1 [BAD13492.1]), low-CO_2-inducible chloroplast membrane Ci candidate transporter (LCIA [XP_001703387.1]), low-CO_2-inducible proteins to recapture leaking CO_2 (LCIB [EDP04243.1], LCIC [BAD16683.1]), chloroplast carrier protein 1 (CCP1 [EDP04147.1]), high light-activated 3 (HLA3) ATP-binding cassette (ABC) transporter (HLA3 [XP_001700040.1]) and chloroplast proton extrusion protein (CemA [XP_001696592]). Retrieved sequences were further subjected to a reciprocal blastx search against the National Center for Biotechnology Information (NCBI) Genbank nonredundant (nr) database. Furthermore, a VecScreen was run on retrieved sequences to check for vector contamination.

Interactive light × CO_2 experimental set-up

Six discs of *U. rigida* clones (each 3 cm^2) were contained in each 24 × 650 mL Perspex flow-through culture vessels. Specimen was pre-incubated under pH_T 7.96 and nutrient replete condition (11.6 ± 0.7 μmol L^{-1} NO_3-N, 9.1 ± 0.4 μmol L^{-1} PO_4-P and 0.6 ± 0.1 μmol L^{-1} NH_4-N; ± SD, n = 3), exposed to PPFR of 30 μmol photons m^{-2} s^{-1} (400–700 nm, 12 h: 12 h, light:dark) inside a temperature-controlled walk-in culture chamber set to 13 ± 1°C. A preliminary rapid ETR-E curve measurement calculated a saturating irradiance E_k = 79 ± 9 μmol

photons m^{-2} s^{-1}, and no photo-inhibition of the maximum electron transport rate (ETR_{max}) was observed up to a maximum PPFR of 600 μmol photons m^{-2} s^{-1} (R. Rautenberger, unpubl. data). Accordingly, two light treatments (PPFR of 400–700 nm) were set as follows: a limiting light (LL) of 31 ± 9 μmol photons m^{-2} s^{-1} and a saturating light (SL) of 274 ± 18 μmol photons m^{-2} s^{-1}. Philips HPI- T 400 W quartz metal halide lamps (Philips) provided the experimental light and the PPFR measured using a 4π quantum sensor (QSL-2101, Biospherical Instruments Inc., San Diego, CA, USA). The LL treatment was achieved using layers of neutral density black screen cover.

The response of *U. rigida* to a shift in pCO_2 was investigated under two treatments slightly higher than today's pCO_2 (471 μatm) and that predicted for year 2100 (1224 μatm). The 160% higher $CO_{2(aq)}$ between the low and high pCO_2 treatments is slightly lower than the 192% increase projected in 2100 (Meehl et al. 2007; IPCC 2013). After three days pre-incubation described above, each culture vessel was randomly assigned to different pCO_2/pH_T (high CO_2/low pH_T 7.59 = HC; low CO_2/high pH_T 7.97 = LC) and light (LL; SL) treatments under higher nitrate concentration (90 μmol L^{-1} NO_3-N). The two factorial experiment resulted in four treatment combinations of light and pCO_2: HC/LL, HC/SL, LC/LL and LC/SL (n = 6).

Manipulation of the seawater carbonate system was achieved using a modified version of the automated pH-controlled culture system described by McGraw et al. (2010). Briefly, target pH (pH_T) levels were achieved by adding HCl and $NaHCO_3$ (Hurd et al. 2009; Riebesell et al. 2010) to the nutrient-enriched seawater and measured spectrophotometrically to an accuracy of 0.03 pH units. Thereafter, the pH-adjusted seawater automatically supplied fresh medium to the respective randomly assigned culture vessel. Seawater in each of the 24 vessels was refreshed every 4.4 h (=4× a day change in medium). Within the 4.4-h incubation period, a maximum 0.18 units increase in pH due to photosynthesis was estimated (Cornwall et al. 2012); thereby persistently exposing the algae to a specific range of the pH treatment. Each culture vessel was provided with water movement using magnetic bars stirred at 650 rpm. Five hundred milliliter of the acid–base manipulated seawater corresponding to pH_T 7.59 and 7.97 was collected and fixed with mercuric chloride. Total alkalinity (A_T) of samples was measured using the closed-cell titration method described by Dickson et al. (2007). A_T, pH, salinity, and temperature were used to calculate carbonate chemistry parameters using the program SWCO2 (Hunter 2007). The seawater carbonate chemistry is presented in Table 1.

Table 1. Summary of carbonate chemistry of seawater used in the experiment.

Parameter (unit)	Ambient CO_2 LC	Elevated CO_2 HC
A_T (μmol kg^{-1})	2197.44 ± 11.99	2207.55 ± 15.97
DIC (μmol kg^{-1})	2031.41 ± 11.23	2170.76 ± 15.74
H_2CO_3 (μmol kg^{-1})	18.49 ± 0.11	48.02 ± 0.51
HCO_3^- (μmol kg^{-1})	1890.43 ± 10.37	2066.36 ± 14.97
CO_3^{2-} (μmol kg^{-1})	122.48 ± 0.88	56.38 ± 0.66
pCO_2 (μatm)	471.38 ± 2.87	1223.91 ± 13.02
pH_T	7.965 ± 0.002	7.590 ± 0.004

Carbonate parameters were calculated from total alkalinity (A_T) and pH_T measurements corresponding to each pCO_2 treatment at 13 ± 1°C. Seawater was filtered and nutrient-enriched (ENSW formula), salinity 34 psu. Data are means ± standard deviations (n = 12).

After 7 days, samples were analyzed for growth, photosynthetic efficiency, pigments, stable isotope signatures, and internal and external carbonic anhydrase (CA) activity. For biochemical analyses, samples were stored either at –20°C (pigment) or –80°C (CA) until analysis.

Growth rate

Algal discs (Fig. 1 inset) from each culture vessel were blotted dry and photographed by a 14-megapixels resolution digital camera (Lumix DMC-FT10; Panasonic, Osaka, Japan). Algal surface area (cm^2) was analyzed by comparing the pixel density of algal discs to a known reference area using the software ImageJ version 1.47b (National Institutes of Health, Bethesda, MD, USA, http://rsb.info.nih.gov/ij/). Relative growth rate (RGR; % d^{-1}) was calculated from the surface area at the start and end of the experiment after Lüning (1990).

Chlorophyll *a* fluorescence

The Chl*a* fluorescence of each algal disc was measured submerged in their respective pH treatment using a PAM-2000 fluorometer (Walz GmbH, Effeltrich, Germany) following the protocol of Rautenberger et al. (2009) at 13 ± 1°C. After 5-min dark incubation, basic (F_0) and maximum fluorescence (F_m) was measured and F_v/F_m was calculated (Schreiber et al. 1995). Electron transport rate (ETR) vs. irradiance (E) curves (ETR–E curves) were recorded from discs exposed to incrementally increasing (every 30 s) actinic light (AL) intensities (7–500 μmol photons m^{-2} s^{-1}; 400–700 nm). All saturation pulses were set to >9000 μmol photons m^{-2} s^{-1} and 0.8 s. The ETRs through the photosystem II (PSII) were calculated by multiplying the intensity of incident AL, the proportion of incident AL intensity that was absorbed by

the measured disc, the fraction of absorbed AL which is most probably received by PSII (0.5) and the PSII operating efficiency (Baker 2008). Maximum electron transport rates (ETR_{max}), the initial slopes of ETR–*E* curves, called α, and the light saturation points of ETRs (i.e., E_k) were estimated from ETRs plotted against the incident AL intensity and calculated according to the model of Jassby and Platt (1976) using the software R version 2.15 (The R Foundation for Statistical Computing, http://www.R-project.org).

Pigments

Frozen algal discs were extracted in 3 mL of 100% N-N-dimethylformamide (DMF; BDH Laboratory Supplies, UK) at 4°C in the dark for 42 h. Chl*a* and Chl*b* were analyzed photometrically at 663.8 and 646.8 nm (Ultrospec 3000; Pharmacia Biotech, Cambridge, UK) with 100% DMF as reference at 20°C. Readings at 750.0 nm were used as a correction for scattering light. Chl*a* and Chl*b* contents were calculated after Porra et al. (1989) and normalized to algal biomass (μg mg^{-1} FW).

Extracellular and intracellular carbonic anhydrase activity

Carbonic anhydrase activity was measured according to the pH drift method of Wilbur and Anderson (1948) and Haglund et al. (1992a) using 50 mmol L^{-1} Tris HCl buffer (adjusted to pH 8.5, 4°C), 2 mmol L^{-1} dithiothreitol (DTT), 15 mmol L^{-1} ascorbic acid and 5 mmol L^{-1} EDTA (disodium salt). The external carbonic anhydrase (CA_{ext}) activity was analyzed from frozen algal discs (60 ± 20 mg FW). Each disc was placed in a 20-mL scintillation vial containing 10 ml of the extraction buffer and equipped with a micro stirrer bar (10 × 3 mm) for the enzymatic reaction. The glass vial was placed inside an ice-containing 100-mL plastic container to maintain the temperature at 0–2°C, sitting on top of a magnetic stirrer to stir the solution. Temperature and pH were simultaneously measured using a ROSS electrode (Orion 8107BNUMD) coupled to Orion 3–Stars Plus pH Benchtop meter (Orion, Thermo Fisher Scientific, Waltham, MA, USA). When pH stabilized at 8.3, 5 mL of ice-cold CO_2-saturated water was added. The time (sec) taken for the pH to drop by 0.4 units, in the pH interval of 8.3–8.1, was recorded. The internal carbonic anhydrase (CA_{int}) activity was subsequently measured from the same algal disc (Fernández et al. 2014). The algal disc was ground to fine powder in liquid N_2-frozen mortar and pestle. The ground tissue (60 ± 20 mg) was analyzed following the protocol described above. Relative enzyme activity (REA) was computed after the formula of Haglund et al. (1992b).

Carbon to nitrogen ratios and stable carbon isotope signatures

Molar C:N ratios and $\delta^{13}C$ signatures (‰) were analyzed after algal discs were dried at 60 ± 1°C for 24 h. Discs were ground in a mortar and pestle to a fine powder and combusted in a CE NA1500 Elemental Analyzer (Carlo-Erba Instruments Ltd, Hindley Green, Wigan, UK) interfaced to an IRMS 20-20 continuous flow mass spectrometer (Europa Scientific Ltd, Crewe, UK). Corrections for drift were made automatically every five samples from an EDTA standard with a known isotope ratio.

Data analyses

Means ± standard deviations (SDs) were calculated from five ($n = 5$) or six ($n = 6$) measurements per treatment. Statistical analyses were performed using JMP Pro 10.0 (SAS Institute Inc., Cary, NC, USA) and R versions 2.7 and 2.15 (The R Foundation for Statistical Computing, http://www.R-project.org). Two-way ANOVA and *t*-test were used to identify statistical differences of the means within and between treatments. Tukey's honestly significant difference (HSD, $P < 0.05$) test was used as a post hoc test.

Results

Carbon physiology and in silico detection of putative CCM from EST libraries

Under pH_T 9.0, initial blocking of the direct HCO_3^- uptake through the AE port by DIDS resulted in 44% inhibition of the net photosynthetic rate (NPS) in *U. rigida*. Subsequent inhibition of the CA_{ext} by AZ to arrest the catalyzed dehydration of HCO_3^- to CO_2 resulted in an additional 39% inhibition of photosynthesis. When the order of inhibition for HCO_3^- use was reversed, AZ and DIDS caused 29% and 26% of the NPS, respectively. Total inhibition of the NPS was higher when direct HCO_3^- uptake through the AE port was blocked first (*T*-test, $P = 0.0195$; Fig. 2). Depending on the order of application of the inhibitors, 17–44% of NPS remained unaccounted.

In the absence of sequence information from *U. rigida*, the search for putative CCM elements in the EST libraries of *U. prolifera* (Jia et al. 2011) identified two α-CA and three γ-CAs (Table S1). However, the putative targeting signal peptides could not be resolved because the sequences retrieved from the EST data were not full length. Moreover, the exact localization of these proteins (e.g. chloroplast or periplasm) could not be defined. No β-CA was found in the EST libraries of

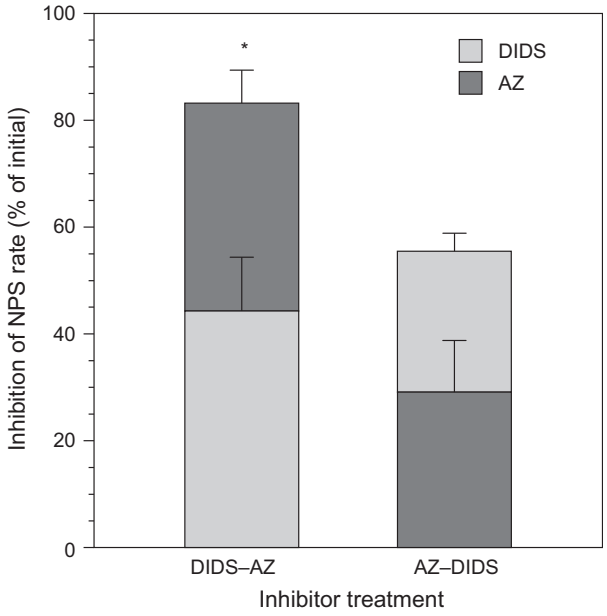

Figure 2. Photosynthetic inhibition after sequential blocking of the anion-exchange (AE) port followed by the inhibition of external carbonic anhydrase (CA_{ext}) activity by 4,4′–diisothiocyanatostilbene–2,2′–disulfonate (DIDS) and acetazolamide (AZ), respectively (= DIDS-AZ), and the reverse order of inhibition: the CA_{ext} activity first, followed by the AE port (= AZ-DIDS). Photosynthesis was measured under pH_T 9. Errors bars, ± SD, n = 3. *, $P < 0.01$.

U. prolifera. Furthermore, four putative HLA3 ABC transporters and three chloroplast carrier proteins (CCP1) and five mitochondrial transporter protein were found (Table S1). The transcriptome of a second species *Ulva linza* also identified putative CCM genes (Zhang et al. 2012). Among those found are at least one α-CA localized in the chloroplast lumen, several low CO_2-induced proteins, a chloroplast Ci transporter (LCIB), several ABC transporters as well as the nuclear transcriptional regulators of CCM elements (CIA5, LCR1).

Growth rate

Relative growth rates (RGR; Fig. 3) of *U. rigida* discs grown under limiting light (LL) were similar under low pCO_2 (LC; 8.5 ± 2.7% d^{-1}) and high pCO_2 (HC; 9.1 ± 3.6% d^{-1}). When discs were exposed to a saturating light (SL), RGRs were 2.27× and 2.35× higher under LC and HC, respectively (Fig. 3). Statistical analysis showed that RGRs were strongly influenced by the experimental irradiance (ANOVA, $P < 0.001$) but not by pCO_2 (ANOVA, $P = 0.2473$). The interaction between irradiance and pCO_2 did not significantly affect the growth rate (ANOVA, $P = 0.5245$).

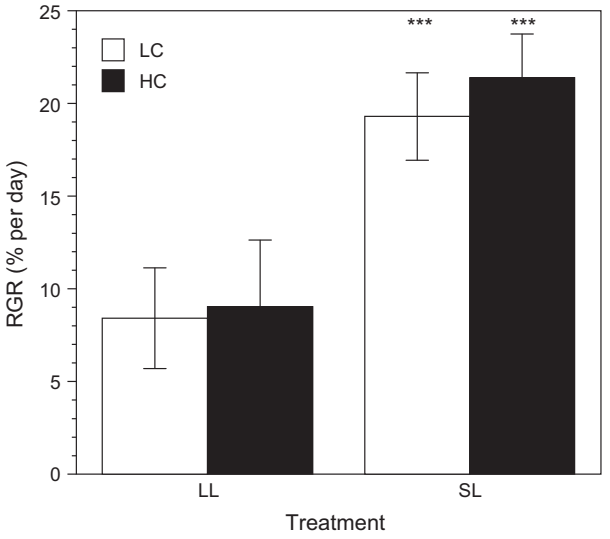

Figure 3. Relative growth rates (RGR) of *Ulva rigida* grown for 7 days under low and high pCO_2 (LC = 471 μatm and HC 1224 μatm, respectively) and limiting and saturating light (LL = 31 μmol photons m^{-2} s^{-1} and SL = 274 μmol photons m^{-2} s^{-1}, respectively). Errors bars, ± SD, n = 6. ***, $P < 0.001$.

Chlorophyll *a* fluorescence

The maximum quantum yield of PSII (F_v/F_m) of *U. rigida* ranged from 0.807 to 0.813 (Table 2). Neither light (ANOVA, $P = 0.152$) nor the seawater carbonate chemistry (ANOVA, $P = 0.391$) or their interaction (ANOVA, $P = 0.593$) had an effect on F_v/F_m.

All electron transport rate-irradiance (ETR-*E*) curve parameters (Table 2), that is, ETR_{max}, E_k and α, were significantly different between light (ANOVA, $P < 0.0001$) but not significantly different between seawater carbonate chemistry (ANOVA, $P > 0.05$). No significant interactive effect of the independent variables was observed in any of the ETR-*E* curve parameter (ANOVA, $P > 0.05$). The ETR_{max} and E_k were significantly higher at saturating light (LL < SL; Tukey's HSD test, $P < 0.05$), while the photosynthetic efficiency, α, was significantly higher at low light (LL > SL; Tukey's HSD test, $P < 0.05$).

Pigments

All LL-grown discs had a significantly higher biomass-based content of both Chl*a* and Chl*b* (Table 2) compared with SL-grown discs (ANOVA, $P < 0.0001$). The content of both chlorophylls was not affected by pCO_2 (ANOVA, $P > 0$ .05). Light and pCO_2 had an interactive effect on both Chl*a* (ANOVA, $P = 0.027$) and Chl*b* (ANOVA, $P = 0.026$). When grown under SL, the Chl*a* content was ∼35% lower than discs grown under LL. Similarly, the Chl*b* content in LL-grown discs was ∼50% higher than

Table 2. Photophysiological parameters and tissue stoichiometry in *Ulva rigida* after seven-day incubation under different pCO_2 and irradiance.

	LL 31 μmol photons m^{-2} s^{-1}		SL 274 μmol photons m^{-2} s^{-1}	
	LC 471 μatm	HC 1224 μatm	LC 471 μatm	HC 1224 μatm
Parameter	pH_T 7.97	pH_T 7.59	pH_T 7.97	pH_T 7.59
F_v/F_m (rel. units)	0.813 ± 0.011	0.821 ± 0.008	0.807 ± 0.010	0.809 ± 0.023
ETR_{max} (μmol electrons m^{-2} s^{-1})	28.9 ± 3.0	30.6 ± 5.6	42.2 ± 1.6	42.8 ± 3.5
E_k (μmol photons m^{-2} s^{-1})	165.5 ± 16.9	169.6 ± 40.6	241.5 ± 9.1	245.3 ± 19.8
α (μmol electrons μmol^{-1} photons)	0.227 ± 0.008	0.227 ± 0.005	0.195 ± 0.012	0.187 ± 0.014
Chl*a* (μg mg^{-1} FW)	1.45 ± 0.27	1.68 ± 0.12	1.09 ± 0.19	0.92 ± 0.21
Chl*b* (μg mg^{-1} FW)	0.88 ± 0.13	0.95 ± 0.05	0.49 ± 0.05	0.42 ± 0.06
Chl*a*/*b*	1.64 ± 0.09	1.76 ± 0.14	2.19 ± 0.22	2.20 ± 0.30
C:N	9.7 ± 0.5	9.6 ± 0.3	10.5 ± 0.7	10.0 ± 0.8

Maximum quantum yield of PSII (F_v/F_m), electron transport rate-irradiance (ETR-*E*) curve parameters, that is, ETR_{max}, E_k, and α estimated using the hyperbolic tangent model of Jassby and Platt (1976), pigments, and molar C:N of *U. rigida* under different light (LL and SL; limiting and saturating light, respectively) and pCO_2 concentrations (LC and HC; low and high pCO_2, respectively). Data are means ± standard deviations (n = 6). FW – fresh weight.

those grown in SL. The highest Chl*a*/*b* ratio of 2.2 (LC and HC) were calculated for SL-grown discs, whereas LL-grown discs had lower ratios of 1.64 (LC) and 1.76 (HC).

Extracellular and intracellular carbonic anhydrase activity

The CA_{ext} activities (Fig. 4A) ranged between 3.54 and 4.28 REA g^{-1} FW and were similar in all treatments (ANOVA, $P > 0.05$), whereas CA_{int} activities (Fig. 4B) were 20% higher under SL compared with LL (ANOVA, $P = 0.002$) irrespective of pCO_2. An increase in pCO_2 (ANOVA, $P = 0.943$) and the interaction between light and pCO_2 (ANOVA, $P = 0.387$) did not significantly change the CA_{int}. Regardless of pCO_2, the CA_{int} was 1.5–2× higher compared with the CA_{ext} under LL and SL, respectively.

Carbon to nitrogen ratios and stable carbon isotope signatures

Molar C:N ratios (Table 2) and $\delta^{13}C$ signatures (Fig. 5) of *U. rigida* differed significantly between light treatment, but there was no effect of seawater carbonate chemistry. Regardless of pCO_2, the molar C:N ratio of LL-grown discs (LC = 9.7 ± 0.5; HC = 9.6 ± 0.3) was significantly lower than those in SL-grown discs (LC= 10.5 ± 0.7; HC = 10.0 ± 0.38; ANOVA, $P = 0.036$; HSD test, $P < 0.05$; LL < SL). Likewise, stable carbon isotope signatures (Fig. 5) of LL-grown discs were similar between LC (–22.12 ± 1.31‰) and HC (–22.32 ± 1.53‰). When algal discs were grown under SL, these signatures shifted to a higher range under LC (–9.76 ± 2.24‰) and HC (–9.78 ± 1.01‰) (ANOVA, $P < 0.001$; HSD test, $P < 0.05$; LL < SL). The interaction between pCO_2 and light did not significantly affect C:N ratio (ANOVA, $P = 0.517$) nor the $\delta^{13}C$ signatures (ANOVA, $P = 0.895$).

Discussion

Our study showed that HCO_3^- is the primary exogenous Ci source used by *Ulva rigida* to support growth and photosynthesis under saturating light, supporting the findings of previous work on other *Ulva* species (e.g. Björk et al. 1992; Drechsler et al. 1993; Larsson et al. 1997). However, when the known HCO_3^- use mechanisms, that is, direct HCO_3^- uptake through the AE port and external catalyzed dehydration of HCO_3^-, in *U. rigida* were inhibited, net photosynthesis (NPS) decreased by only 56–83% leaving the carbon uptake mechanism(s) for the remaining 17–44% of NPS unaccounted for. The remaining production cannot be attributed $CO_{2(aq)}$ as the concentrations under pH_T 9.0 are much too low but rather to a possible light-dependent active HCO_3^- transport system. An in silico search of EST libraries of *U. prolifera* (Jia et al. 2011) found putative light-dependent HCO_3^- transporters, that is, the ABC transporters of the ABCC subfamily also found in *U. linza* (Zhang et al. 2012), which resemble the HLA3 transporter found in *Chlamydomonas* (Meyer and Griffiths 2013). The ABCC transporters are present in all eukaryotes and have different transport functions, including vacuolar sequestration of toxic metabolites and transport of chlorophyll catabolites during senescence, among others (Meyer and Griffiths 2013). The HLA3 analog has been implicated in the active bicarbonate uptake in *Chlamydomonas*: their role in

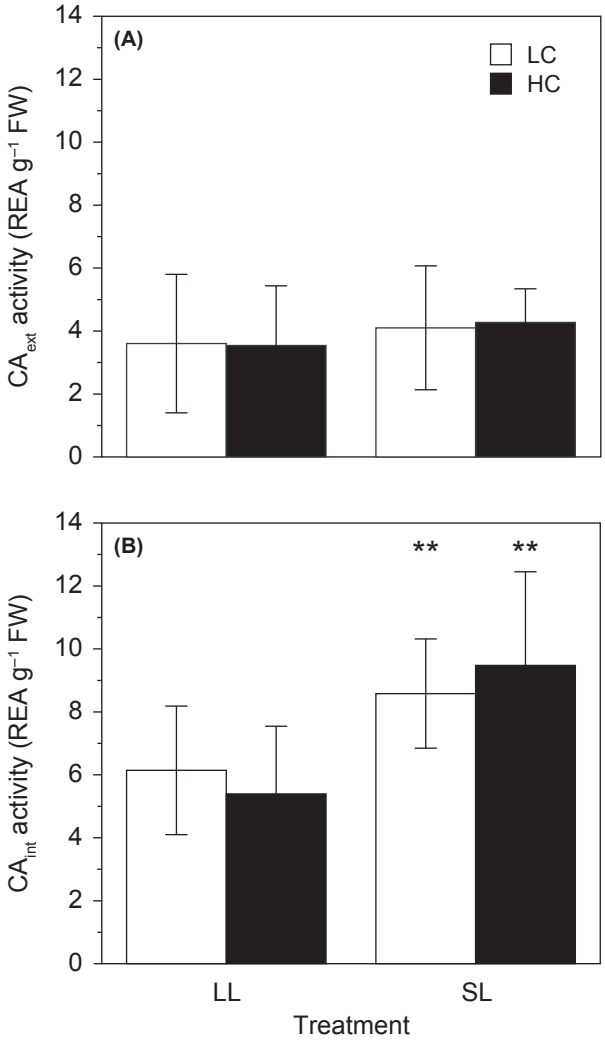

Figure 4. Relative enzyme activity (REA) of external (A) and internal (B) carbonic anhydrase activities in *Ulva rigida* after 7 days incubation under low and high pCO_2 (LC = 471 μatm and HC 1224 μatm, respectively) and limiting and saturating light (LL = 31 μmol photons m^{-2} s^{-1} and SL = 274 μmol photons m^{-2} s^{-1}, respectively). Errors bars, ± SD, n = 6. **, $P < 0.01$.

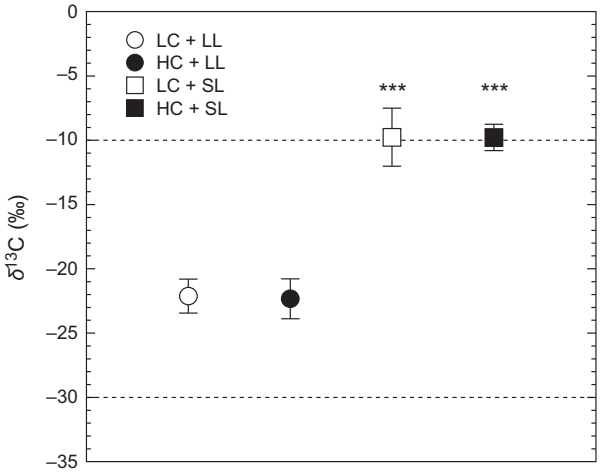

Figure 5. Stable carbon isotope signatures ($\delta^{13}C$) of *Ulva rigida* after seven-day incubation under low and high pCO_2 (LC = 471 μatm and HC 1224 μatm, respectively) and limiting and saturating light (LL = 31 μmol photons m^{-2} s^{-1} and SL = 274 μmol photons m^{-2} s^{-1}, respectively). Horizontal lines delimit the possible values for inorganic carbon use, that is, wholly dependent on CO_2 (<−30‰) or HCO_3^- (>−10‰); values in between suggest mix use of CO_2 and HCO_3^- (*cf* Roleda and Hurd 2012). Errors bars, ± SD, n = 6. ***, $P < 0.001$.

a CCM is supported by genetic and physiological evidence (Wang et al. 2011).

Several CAs are involved in the utilization of HCO_3^-. For example, the α-CAs, pCA1 and pCA2, catalyze the external dehydration of HCO_3^- in *Chlamydomonas* (Spalding 1998); however, these isozymes are not found in *Ulva*. An unclassified CA_{ext} isozyme may be present in *Ulva*, but their contribution to the external dehydration of HCO_3^- to CO_2 and the active and/or passive transport of CO_2 into the cell may not be sufficient to supply and fill the internal Ci pool to support the high growth rate of the species. Instead, two putative intracellular α-CA isozymes were found in the EST libraries of *U. prolifera* (Jia et al. 2011). These α-type CA isozymes also identified in *U. linza* (Zhang et al. 2012) most likely have a subcellular localization, for example, the chloroplast lumen. Both studies, that is, Zhang et al. (2012) and Ye et al. (2014), suggest that this α-CA isozyme is responsible for the internal HCO_3^- dehydration to provide the chloroplast with sufficient CO_2 for carbon fixation. The same was recently reported in *Saccharina japonica*, where cDNA encoding α-CA was associated with the chloroplast envelopes and thylakoid membranes (Ye et al. 2014). Although the β-type CA was not found in the EST of *Ulva*, it is reported to be localized in the cytosol of another green alga *Coccomyxa* (Huang et al. 2011) where it facilitates Ci diffusion from the inner surface of the plasmalemma to the chloroplast envelope.

On the other hand, the exact roles of γ-type CA identified in the ESTs of *U. prolifera* are still unknown. They are usually associated with the mitochondria of green algae and plants (Parisi et al. 2004). Mitochondrial carbonic anhydrase (mtCA) is involved in enzymatic hydration of CO_2, produced during respiration and photorespiration, to HCO_3^- to stimulate anaplerotic β-carboxylation, where sufficient supply of HCO_3^- is required to support nonphotosynthetic biosynthetic pathways (Giordano et al. 2003). This may explain the nonphotosynthetic growth enhancement reported in *U. rigida* (Gordillo et al. 2001). This mechanism that recovers respiratory CO_2 presents a very effective way to ensure efficient use of Ci for photosynthesis and nonphotosynthetic Ci-use pathways

specially among calcifying algae and invertebrates (Roleda et al. 2012b).

The role of CA_{ext} in the Ci use of *U. rigida* was insignificant and was not regulated by either pCO_2 or light. Despite the 160% increase in CO_2 under the HC treatment (1224 μatm), downregulation in CA_{ext} activity was not observed, a finding opposite to those found in the microalga *Emiliania huxleyi* (Richier et al. 2011). The constant low CA_{ext} activities (3.54–4.28 REA g^{-1} FW) across all treatments suggest that CO_2 uptake after catalyzed external dehydration of HCO_3^- is not the main source of Ci in *U. rigida*. Considering that diffusive entry of aqueous CO_2 into the cell is very slow in water, this mechanism is deemed to be insufficient for the accumulation of an internal Ci pool large enough to support the observed high growth rates (max 20% d^{-1}) in this species. Moreover, CO_2 uptake requires a conversion of CO_2 to HCO_3^- to maintain internal pH and avoid CO_2 leakage from the cell (Price et al. 2008).

Conversely, CA_{int} was 1.5–2× higher under saturating light compared with limiting light. The higher enzymatic activity facilitates the conversion of HCO_3^- to CO_2 to support the higher CO_2 requirement of RuBisCO for photosynthetic fixation driving higher growth rate under saturating light. However, the source of this internal Ci pool (under high pH 9.0) cannot be wholly attributed to the known HCO_3^- uptake mechanism where only up to 44% of net photosynthesis is supported by the direct HCO_3^- uptake through the AE port and 39% by the CA_{ext}-mediated HCO_3^- dehydration. The light-dependent HLA3 ABC transporters described above are hypothesized to most likely contribute to direct HCO_3^- transport in order to saturate the internal Ci pool. HCO_3^- is the preferred Ci form for cellular accumulation because it is about 1000-fold less permeable to lipid membranes than CO_2 (Price et al. 2008).

When active HCO_3^- transport through the AE port was blocked first, inhibition of NPS during the 15-min period was 34% higher than when CA_{ext}-mediated HCO_3^- use was blocked first. Subsequent application of the second inhibitor contributed to additional 39% and 26% for the DIDS-AZ and AZ-DIDS treatment, respectively. In the AZ-DIDS treatment, where the CA_{ext}-mediated HCO_3^- use was initially inhibited, algal discs were still actively transporting HCO_3^- through the AE port that enables the cells to accumulate higher internal Ci pool contributing to lesser total inhibition of NPS. Conversely, when active HCO_3^- transport through the AE port was blocked first (DIDS-AZ), significantly higher total inhibition of NPS was observed. This suggests that different HCO_3^- use mechanisms operate simultaneously and that the active transport through the AE port contributes more Ci to the internal pool.

Earlier studies of the carbon physiology of different *Ulva* species that focused on the AE port and external dehydration of HCO_3^- reported contradictory results. Larsson and Axelsson (1999) reported the net photosynthetic rates of different *Ulva* species are primarily supported by external dehydration of HCO_3^- (34–68%) rather than direct HCO_3^- uptake (9–40%) through the AE port. Another study by Axelsson et al. (1999) reported >90% of *Ulva lactuca* photosynthesis is dependent on AZ-sensitive HCO_3^- dehydration mechanism. Drechsler and Beer (1991) and Drechsler et al. (1993) reported a significantly higher contribution of direct HCO_3^- uptake compared with CA_{ext}-catalyzed HCO_3^- dehydration in *U. lactuca*. The above-mentioned studies on HCO_3^- use mechanisms was measured between pH 8.2 and pH 8.7. At pH >9.4, only HCO_3^- uptake via the putative DIDS-sensitive AE-transporter is operational in *Ulva intestinalis* (formerly *Enteromorpha intestinalis*) (Larsson et al. 1997). Conversely, only at extremely low pH 5.6 was a higher affinity for CO_2 observed, which had no adverse effect on *U. lactuca*'s photosynthetic performance (Drechsler and Beer 1991). It should be noted that those *Ulva* species reported above may have some degree of taxonomical uncertainty. Previous physiological studies on *Ulva* did not identify that a light-dependent HCO_3^- transporter is most likely operational in *Ulva*'s CCM as found in this study.

Elevated Ci (both CO_2 and HCO_3^-) under OA did not cause a higher growth in *U. rigida* but growth rate was limited by light. This suggests that the present-day Ci concentration is already saturating for *Ulva*. Cyanobacterial ancestors of the green algae evolved effective HCO_3^- use mechanisms during the geologic low-CO_2 environment (Giordano et al. 2005); we suggest that this trait is most likely genetically fixed and the modern *Ulva* can modulate their CCM under different pCO_2 conditions (Giordano et al. 2005). Our results do not support the observation of Gordillo et al. (2001) on the same species and Xu and Gao (2012) on *U. prolifera* that higher pCO_2 causes an increase in rates of both photosynthesis and growth. Although the response may be species specific, the mechanistic study of Gordillo et al. (2001) used extremely high CO_2 in air (10 000 μL L^{-1}) and the identity of their *U. rigida* is uncertain as this was not molecularly identified (F. J. L. Gordillo, pers. comm.). The results of our study concur with those of Drechsler and Beer (1991) on *U. lactuca* where maximum photosynthetic O_2 evolution was comparable under low (5.6) and high (8.2) pH. Furthermore, the study of Mercado et al. (2001) on the carbon physiology of three red seaweeds of the order Gelidiales inhabiting the intertidal zone also reported that photosynthesis is limited by light and not by Ci availability.

The seawater Ci species, that is, CO_2 and HCO_3^-, used as substrate for carbon uptake and fixation consist of stable carbon isotopes ^{13}C and ^{12}C within each species. The present seawater consist of 1% CO_2 and 91% HCO_3^-; of all natural carbon, only 1.1% is ^{13}C while 98.89% is ^{12}C. Relative to $^{13}\delta_{VPDB}$ standard, $CO_{2(aq)}$ has $\delta^{13}C = -10‰$ while dissolved HCO_3^- has $\delta^{13}C = +1‰$ to $+1.5‰$ (Mook et al. 1974; Mook 2005). The $^{13}C/^{12}C$ ratios (= $\delta^{13}C$) of the organic cellular material has been used as a proxy of Ci use relative to bulk seawater Ci source (Giordano et al. 2005). For example, organisms with $\delta^{13}C$ higher than $-10‰$ (a value more positive than $\delta^{13}C$ of CO_2 in seawater) must involve HCO_3^- use (Raven et al. 2002). Among mixed CO_2/HCO_3^- using algae, a significant use of CO_2 under high pCO_2 will shift $\delta^{13}C$ signature corresponding to more CO_2 use (i.e. toward $-30‰$) (Maberly et al. 1992). Here, we found that regardless of pCO_2, $\delta^{13}C$ signatures of *U. rigida* shifted upwards toward values of $-10‰$ and higher, under saturating light, which provides further support of the presence of a light-dependent active HCO_3^- transport and intracellular accumulation, and the use of available HCO_3^- to support photosynthetic carbon fixation as previously suggested by Raven et al. (2002).

The C-isotope fractionation in aquatic plants is more complex than in terrestrial plants (Hoefs 2009). Factors that control the $\delta^{13}C$ signature in algae include not only the availability of $CO_{2(aq)}$, but also temperature, light intensity, nutrient availability, pH, and physiological factors such as cell size and growth rate (Hoefs 2009 and references therein). In *U. rigida*, the increase in productivity observed under saturating light regardless of increased availability of $CO_{2(aq)}$ causes a corresponding rise in $\delta^{13}C$ values, a response associated with more ^{12}C locked up in the tissue as organic matter is generally depleted in ^{13}C (Zeebe and Wolf-Gladrow 2001).

Moreover, the carbon fixation pathway can also influence the isotopic composition of organic matter. $\delta^{13}C$ signatures between –32% and –22% are characteristics of C_3 plants while $\delta^{13}C$ between $-16‰$ and $-10‰$ are typical for C_4 plants (Zeebe and Wolf-Gladrow 2001; Hoefs 2009 and references therein). The natural variations in the $\delta^{13}C$ signature of *U. rigida* between $-22‰$ and $-10‰$ point to the possible occurrence of a C_4 photosynthetic carbon fixation pathway, as observed in *U. linza* (Xu et al. 2013).

The rising atmospheric CO_2 does not only trigger OA but also contributes to global warming that strengthens the vertical stratification of aquatic ecosystems: this suppresses the nutrient supply from deep water into the surface layer. The enhanced CO_2 but reduced nutrient supply can therefore increase the C:N ratio of primary producers (e.g., phytoplankton) which are of low nutritional value to consumers (e.g., zooplankton), cascading throughout the entire aquatic food web (van de Waal et al. 2010). In our experiment, we increased CO_2 by ~160% and HCO_3^- by ~9% while the nutrient level remained constant. In this scenario, the enhanced exogenous Ci concentration and constant nutrient supply will theoretically still increase the C:N ratio. However, the insignificant fractional increase was observed relative to light and not to CO_2 (Table 2). This suggests that changes in the tissue/cellular stoichiometry in macroalgae may not be sensitive to a change in Ci alone. The small increase in C:N under saturating light suggests that exogenous Ci concentration is already saturating for *Ulva* regardless of pCO_2 and saturating light increase carbon fixation.

The maximum quantum yield of PSII (F_v/F_m) and other photosynthetic parameters (ETR_{max}, E_k, α) are reliable proxies to assess seaweed photosynthetic performance under environmental stress such as high PAR, UVR, and temperature (e.g., Roleda et al. 2005; Rautenberger and Bischof 2006; Hanelt and Roleda 2009; Rautenberger et al. 2009; Roleda 2009). However, we suggest that these parameters are unlikely to be sensitive to changes in seawater carbonate chemistry, that is, pCO_2 and H^+, within the range likely to occur due to OA. In this study, rigorous PAM-based photophysiological measurements on *U. rigida* showed that ETR_{max}, E_k, and α are regulated by light, and a reduced seawater pH, simulating OA, had no effect, a finding contrary to that of Olischläger et al. (2013). Moreover, and contrary to the reported decrease in chlorophyll pigments under OA in *U. prolifera* (Xu and Gao 2012), OA did not affect the photosynthetic pigments of *U. rigida*: the amounts of Chl*a* and Chl*b* were regulated by light.

Algae regulate internal pH maintaining cytoplasmic pH at 7.3 ± 0.2 (Ritchie 1985; Lundberg et al. 1989; Smith and Bidwell 1989) which is 0.7 units lower than that of the current average surface seawater pH. Moreover, PSII is located in the thylakoid membrane where it is exposed to the acidified lumen (pH 5.0) and neutral to slightly basic stroma (pH 7.2–8.0) (Falkowski and Raven 2007). Therefore, the photosynthetic apparatus is already acclimated to a wide range of pH. The mechanism of how the bulk water pH may affect F_v/F_m is unknown; studies reporting positive or negative effects of OA on this physiological proxy should therefore be interpreted with caution as they are possible artifacts.

In conclusion, *U. rigida* is insensitive to OA. The present-day seawater Ci pool is saturating for photosynthesis and growth, and these parameters were primarily controlled by light rather than elevated $CO_{2(aq)}$. For photosynthetic carbon fixation, HCO_3^- is the primary Ci species assimilated by *U. rigida*. Aside from the known catalyzed external HCO_3^- dehydration and direct HCO_3^- uptake

through the AE port, another inhibitor-insensitive HCO_3^- transport mechanism is most likely present. An in silico search of CCM elements in EST libraries of *Ulva* found putative light-dependent HCO_3^- transporters, that is, the ABC transporters of the ABCC subfamily, found in both *U. prolifera* and *U. linza*. Neither a downregulation in extracellular CA-mediated HCO_3^- dehydration nor a shift to CO_2 use was observed under high $CO_{2(aq)}$. The shift in $\delta^{13}C$ signatures in *U. rigida* toward –10‰ under saturating light under low and high $CO_{2(aq)}$ but not toward –30‰ under elevated $CO_{2(aq)}$ suggests preference and substantial internal HCO_3^- accumulation to support photosynthesis and growth regardless of CO_2 concentrations. Despite the limited effect of OA and PPFR, the interaction of OA with other climate change stressors, for example, eutrophication and warming, may elicit different effects and warrants further investigation.

Acknowledgments

The following research grants are acknowledged for supporting this work: the German Research Foundation (DFG: RA 2030/1-1) to RR; a University of Otago Research Grant to CLH and RR and the Royal Society of New Zealand Marsden Fund (UOO0914) to CLH. SH acknowledges funding from the Beaufort Marine Research Award carried out under the Irish Sea Change Strategy and the Strategy for Science Technology and Innovation (2006–2013), with the support of the Marine Institute, funded under the Marine Research Sub-Programme of the Irish National Development Plan 2007–2013. We are grateful to Katja Schweikert for collecting the *Ulva* specimen.

Conflict of Interest

None declared.

References

Aldridge, J. N., and M. Trimmer. 2009. Modelling the distribution and growth of 'problem' green seaweed in the Medway estuary, UK. Hydrobiologia 629:107–122.

Axelsson, L., H. Ryberg, and S. Beer. 1995. Two modes of bicarbonate utilization in the marine green macroalga *Ulva lactuca*. Plant, Cell Environ. 18:439–445.

Axelsson, L., C. Larsson, and H. Ryberg. 1999. Affinity, capacity and oxygen sensitivity of two different mechanisms for bicarbonate utilization in *Ulva lactuca* L. (Chlorophyta). Plant, Cell Environ. 22:969–978.

Axelsson, L., J. M. Mercado, and F. L. Figueroa. 2000. Utilization of HCO_3- at high pH by the brown macroalga *Laminaria saccharina*. Eur. J. Phycol. 35:53–59.

Baker, N. R. 2008. Chlorophyll fluorescence: a probe of photosynthesis in vivo. Annu. Rev. Plant Biol. 59:89–113.

Beer, T., A. Israel, Y. Helman, and A. Kaplan. 2008. Acidification and CO_2 production in the boundary layer during photosynthesis in *Ulva rigida* (Chlorophyta) C Agardh. Isr. J. Plant Sci. 56:55–60.

Berges, J. A., D. J. Franklin, and P. J. Harrison. 2001. Evolution of an artificial seawater medium: improvements in enriched seawater, artificial water over the last two decades. J. Phycol. 37:1138–1145.

Björk, M., K. Haglund, Z. Ramazanov, G. García-Reina, and M. Pedersén. 1992. Inorganic-carbon assimilation in the green seaweed *Ulva rigida* C.Ag. (Chlorophyta). Planta 187:152–156.

Björk, M., K. Haglund, Z. Ramazanov, and M. Pedersén. 1993. Inducible mechanisms for HCO_3^- utilization and repression of photorespiration in protoplasts and thalli of three species of *Ulva* (Chlorophyta). J. Phycol. 29:166–173.

Boguski, M. S., T. M. J. Lowe, and C. M. Tolstoshev. 1993. dbEST – database for "expressed sequence tags". Nat. Genet. 4:332–333.

Cook, C. M., T. Lanaras, and B. Colman. 1986. Evidence for bicarbonate transport in species of red and brown macrophytic marine algae. J. Exp. Bot. 37:977–984.

Cornwall, C. E., C. D. Hepburn, D. W. Pritchard, C. M. McGraw, K. I. Currie, K. A. Hunter, et al. 2012. Carbon-use strategies in macroalgae: differential responses to lowered pH and implications for ocean acidification. J. Phycol. 48:137–144.

Coutinho, R., and R. Zingmark. 1993. Interactions of light and nitrogen on photosynthesis and growth of the marine macroalga *Ulva curvata* (Kützing) De Toni. J. Exp. Mar. Biol. Ecol. 167:11–19.

Dickson, A. G., C. L. Sabine, and J. R. Christian. 2007. P. 191. Guide to the best practices for ocean CO_2 measurements. PICES Special Publication, 3. North Pacific Marine Science Organization, Sidney, Canada.

Drechsler, Z., and S. Beer. 1991. Utilization of inorganic carbon by *Ulva lactuca*. Plant Physiol. 97:1439–1444.

Drechsler, Z., R. Sharkia, Z. I. Cabantchik, and S. Beer. 1993. Bicarbonate uptake in the marine macroalga *Ulva* sp. is inhibited by classical probes of anion exchange by red blood cells. Planta 191:34–40.

Falkowski, P. G., and J. A. Raven. 2007. P. 484. Aquatic photosynthesis. Princeton Univ. Press, Princeton, NJ.

Fernández, P. A., C. L. Hurd, and M. Y. Roleda. 2014. Bicarbonate uptake via an anion exchange protein is the main mechanism of inorganic carbon acquisition by the giant kelp *Macrocystis pyrifera* (Laminariales, Phaeophyceae) under variable pH. J. Phycol. 50:998–1008.

García, H. E., and L. I. Gordon. 1992. Oxygen solubility in seawater: better fitting equations. Limnol. Oceanogr. 37:1307–1312.

Gattuso, J.-P., and L. Hansson. 2011. P. 352. Ocean acidification. Oxford Univ. Press, Oxford, UK.

Giordano, M., A. Norici, M. Forssen, M. Eriksson, and J. A. Raven. 2003. An anaplerotic role for mitochondrial carbonic anhydrase in *Chlamydomonas reinhardtii*. Plant Physiol. 132:2126–2134.

Giordano, M., J. Beardall, and J. A. Raven. 2005. CO_2 concentrating mechanisms in algae: mechanisms, environmental modulation, and evolution. Annu. Rev. Plant Biol. 56:99–131.

Gordillo, F. J. L., F. X. Niell, and F. L. Figueroa. 2001. Non-photosynthetic enhancement of growth by high CO_2 level in the nitrophilic seaweed *Ulva rigida* C. Agardh (Chlorophyta). Planta 213:64–70.

Guiry, M. D., and G. M. Guiry. 2014. AlgaeBase. Available at http://www.algaebase.org. (accessed 29 March 2014).

Haglund, K., M. Björk, Z. Ramazanov, G. García-Reina, and M. Pedersén. 1992a. Role of carbonic anhydrase in photosynthesis and inorganic-carbon assimilation in the red alga *Gracilaria tenuistipitata*. Planta 187:275–281.

Haglund, K., Z. Ramazanov, M. Mtolera, and M. Pedersén. 1992b. Role of external carbonic anhydrase in light-dependent alkalization by *Fucus serratus* L. and *Laminaria saccharina* (L.) Lamour. (Phaeophyta). Planta 188:1–6.

Hanelt, D., and M. Y. Roleda. 2009. UVB radiation may ameliorate photoinhibition in specific shallow-water tropical marine macrophytes. Aquat. Bot. 91:6–12.

Harrison, P. J., R. E. Waters, and F. J. R. Taylor. 1980. A broad spectrum artificial seawater medium for coastal and open ocean phytoplankton. J. Phycol. 16:28–35.

Hayden, H. S., and J. R. Waaland. 2004. A molecular systematic study of *Ulva* (Ulvaceae, Ulvales) from the northeast Pacific. Phycologia 43:364–382.

Heesch, S., J. E. S. Broom, K. F. Neill, T. J. Farr, J. L. Dalen, and W. A. Nelson. 2009. *Ulva*, *Umbraulva* and *Gemina*: genetic survey of New Zealand taxa reveals diversity and introduced species. Eur. J. Phycol. 44:143–154.

Herfort, L., B. Thake, and J. Roberts. 2002. Acquisition and use of bicarbonate by *Emiliania huxleyi*. New Phytol. 156:427–436.

van Hille, R., M. Fagan, L. Bromfield, and R. Pott. 2014. A modified pH drift assay for inorganic carbon accumulation and external carbonic anhydrase activity in microalgae. J. Appl. Phycol. 26:377–385.

Hoefs, J. 2009. P. 285. Stable isotope geochemistry. Springer, Berlin Heidelberg.

Huang, S., T. Hainzl, C. Grundström, C. Forsman, G. Samuelsson, and A. E. Sauer-Eriksson. 2011. Structural studies of β-carbonic anhydrase from the green alga *Coccomyxa*: inhibitor complexes with anions and acetazolamide. PLoS ONE 6:e28458.

Hunter, K. A. 2007. SWCO2. Available at http://neon.otago.ac.nz/research/mfc/people/keith_hunter/software/swco2/. (accessed 5 October 2011).

Hurd, C. L., C. D. Hepburn, K. I. Currie, J. A. Raven, and K. A. Hunter. 2009. Testing the effects of ocean acidification on algal metabolism: considerations for experimental designs. J. Phycol. 45:1236–1251.

IPCC. 2013. Climate Change 2013: The Physical Science Basis. Contribution of Working Group I to the Fifth Assessment Report of the Intergovernmental Panel on Climate Change. P. 1535 *in* T. F. Stocker, D. Qin, G.-K. Plattner, M. Tignor, S. K. Allen, J. Boschung, A. Nauels, Y. Xia, V. Bex, and P. M. Midgley, eds. Cambridge Univ. Press, Cambridge, UK and New York, NY.

Jassby, A. D., and T. Platt. 1976. Mathematical formulation of the relationship between photosynthesis and light for phytoplankton. Limnol. Oceanogr. 21:540–547.

Jia, S., X. Wang, G. Liu, D. Luo, J. Zhang, Y. Liu, et al. 2011. Gene expression analysis of "green tide" alga *Ulva prolifera* (Chlorophyta) in China. Genes Genomics 33:173–178.

Koch, M., G. Bowes, C. Ross, and X.-H. Zhang. 2013. Climate change and ocean acidification effects on seagrasses and marine macroalgae. Global Change Biol. 19:103–132.

Koeman, R. P. T., and C. van den Hoek. 1981. The taxonomy of *Ulva* (Chlorophyceae) in The Netherlands. Brit. Phycol. J. 16:9–53.

Kübler, J. E., A. M. Johnston, and J. A. Raven. 1999. The effects of reduced and elevated CO_2 and O_2 on the seaweed *Lomentaria articulata*. Plant, Cell Environ. 22:1303–1310.

Larsson, C., and L. Axelsson. 1999. Bicarbonate uptake and utilization in marine macroalgae. Eur. J. Phycol. 34:79–86.

Larsson, C., L. Axelsson, H. Ryberg, and S. Beer. 1997. Photosynthetic carbon utilization by *Enteromorpha intestinalis* (Chlorophyta) from a Swedish rockpool. Eur. J. Phycol. 32:49–54.

Loughnane, C. J., L. M. McIvor, F. Rindi, D. B. Stengel, and M. D. Guiry. 2008. Morphology, *rbc*L phylogeny and distribution of distromatic *Ulva* (Ulvophyceae, Chlorophyta) in Ireland and southern Britain. Phycologia 47:416–429.

Lundberg, P., R. G. Weich, P. Jensén, and H. J. Vogel. 1989. Phosphorus-31 and nitrogen-14 NMR studies of the uptake of phosphorus and nitrogen compounds in the marine macroalgae *Ulva lactuca*. Plant Physiol. 89:1380–1387.

Lüning, K. 1990. P. 544. Seaweeds: their environment, biogeography, and ecophysiology. John Wiley & Sons, New York, NY.

Maberly, S. C., J. A. Raven, and A. M. Johnston. 1992. Discrimination between ^{12}C and ^{13}C by marine plants. Oecologia 91:481–492.

McGlathery, K. J. 2001. Macroalgal blooms contribute to the decline of seagrass in nutrient-enriched coastal waters. J. Phycol. 37:453–456.

McGraw, C. M., C. E. Cornwall, M. R. Reid, K. I. Currie, C. D. Hepburn, P. Boyd, et al. 2010. An automated pH-controlled culture system for laboratory-based ocean acidification experiments. Limnol. Oceanogr. Methods 8:686–694.

Meehl, G. A., T. F. Stocker, W. D. Collins, P. Friedlingstein, A. T. Gaye, J. M. Gregory, et al. 2007. Global climate projections. Pp. 747–845 *in* S. Solomon, D. Qin, M. Manning, Z. Chen, M. Marquis, K. B. Averyt, M. Tignor, and H. L. Miller, eds. Climate change 2007: the physical science basis. Contribution of working group I to the fourth assessment report of the intergovernmental panel on climate change. Cambridge Univ. Press, Cambridge, UK and New York, NY.

Mercado, J. M., F. X. Niell, and M. C. Gil-Rodríguez. 2001. Photosynthesis might be limited by light, not inorganic carbon availability, in three intertidal Gelidiales species. New Phytol. 149:431–439.

Meyer, M., and H. Griffiths. 2013. Origins and diversity of eukaryotic CO_2-concentrating mechanisms: lessons for the future. J. Exp. Bot. 64:769–786.

Millero, F. J., and A. Poisson. 1981. International one-atmosphere equation of state of seawater. Deep-Sea Res. 28:625–629.

Mook, W. G. 2005. P. 226. Introduction to isotope hydrology. Stable and radioactive isotopes of hydrogen, oxygen and carbon. Taylor and Francis/Balkema, Leiden, the Netherlands.

Mook, W. G., J. C. Bommerson, and W. H. Staverman. 1974. Carbon isotope fractionation between dissolved bicarbonate and gaseous carbon dioxide. Earth Planet. Sci. Lett. 22:169–176.

Olischläger, M., I. Bartsch, L. Gutow, and C. Wiencke. 2013. Effects of ocean acidification on growth and physiology of *Ulva lactuca* (Chlorophyta) in a rockpool-scenario. Phycol. Res. 61:180–190.

Pajusalu, L., G. Martin, A. Põllumäe, and T. Paalme. 2013. Results of laboratory and field experiments of the direct effect of increasing CO_2 on net primary production of macroalgal species in brackish-water ecosystems. Proc. Eston. Acad. Sci. 62:148–154.

Pang, S. J., F. Liu, T. F. Shan, N. Xu, Z. H. Zhang, S. Q. Gao, et al. 2010. Tracking the algal origin of the *Ulva* bloom in the Yellow Sea by a combination of molecular, morphological and physiological analyses. Mar. Environ. Res. 69:207–215.

Parisi, G., M. Perales, M. S. Fornasari, A. Colaneri, N. Gónzalez-Schain, D. Gómez-Casati, et al. 2004. Gamma carbonic anhydrases in plant mitochondria. Plant Mol. Biol. 55:193–207.

Porra, R. J., W. A. Thompson, and P. E. Kriedemann. 1989. Determination of accurate extinction coefficients and simultaneous equations for assaying chlorophylls *a* and *b* extracted with four different solvents: verification of the concentration of chlorophyll standards by atomic absorption spectroscopy. Biochim. Biophys. Acta 975:384–394.

Price, G. D., M. R. Badger, F. J. Woodger, and B. M. Long. 2008. Advances in understanding the cyanobacterial CO_2-concentrating-mechanism (CCM): functional components, Ci transporters, diversity, genetic regulation and prospects for engineering into plants. J. Exp. Bot. 59:1441–1461.

Rautenberger, R., and K. Bischof. 2006. Impact of temperature on UV-susceptibility of two *Ulva* (Chlorophyta) species from Antarctic and Subantarctic regions. Polar Biol. 29:988–996.

Rautenberger, R., A. Mansilla, I. Gómez, C. Wiencke, and K. Bischof. 2009. Photosynthetic responses to UV-radiation of intertidal macroalgae from the Strait of Magellan (Chile). Rev. Chil. Hist. Nat. 82:43–61.

Raven, J. A. 1991. Physiology of inorganic C acquisition and implications for resource use efficiency by marine phytoplankton- relation to increased CO_2 and temperature. Plant, Cell Environ. 8:779–794.

Raven, J. A., A. M. Johnston, J. E. Kübler, R. Korb, S. G. McInroy, L. L. Handley, et al. 2002. Mechanistic interpretation of carbon isotope discrimination by marine macroalgae and seagrasses. Funct. Plant Biol. 29:355–378.

Richier, S., S. Fiorini, M. E. Kerros, P. von Dassow, and J.-P. Gattuso. 2011. Response of the calcifying coccolithophore *Emiliania huxleyi* to low pH/high pCO_2: from physiology to molecular level. Mar. Biol. 158:551–560.

Riebesell, U., V. J. Fabry, L. Hansson, and J.-P. Gattuso. 2010. Guide to best practices for ocean acidification research and data reporting. P. 260. Publications Office of the European Union, Luxembourg.

Ritchie, R. J. 1985. Energetic considerations of ion transport in *Enteromorpha intestinalis* (L.) Link. New Phytol. 100:5–24.

Roleda, M. Y. 2009. Photosynthetic response of Arctic kelp zoospores exposed to radiation and thermal stress. Photochem. Photobiol. Sci. 8:1302–1312.

Roleda, M. Y., and C. L. Hurd. 2012. Seaweed responses to ocean acidification. Pp. 407–431 *in* C. Wiencke and K. Bischof, eds. Seaweed Biology. Springer, Berlin, Germany.

Roleda, M. Y., C. Wiencke, D. Hanelt, W. H. van de Poll, and A. Gruber. 2005. Sensitivity of Laminariales zoospores from Helgoland to ultraviolet and photosynthetically active radiation: implications on depth distribution and reproductive season. Plant, Cell Environ. 28:466–479.

Roleda, M. Y., J. N. Morris, C. M. McGraw, and C. L. Hurd. 2012a. Ocean acidification and seaweed reproduction: increased CO_2 ameliorates the negative effect of lowered pH on meiospore germination in the giant kelp *Macrocystis pyrifera* (Laminariales, Phaeophyceae). Global Change Biol. 18:854–864.

Roleda, M. Y., P. W. Boyd, and C. L. Hurd. 2012b. Before ocean acidification: calcifier chemistry lessons. J. Phycol. 48:840–843.

Schreiber, U., W. Bilger, and C. Neubauer. 1995. Chlorophyll fluorescence as a nonintrusive indicator for rapid assessment of in vivo photosynthesis. Pp. 49–70. *in* E.-D. Schulze and M. M. Caldwell, eds. Ecophysiology of photosynthesis. Springer, Berlin, Germany.

Sharkia, R., S. Beer, and Z. I. Cabantchik. 1994. A membrane-located polypeptide of *Ulva* sp. which may be involved in HCO_3^- uptake is recognized by antibodies raised against the human red-blood-cell anion-exchange protein. Planta 194:247–249.

Smith, R. G., and R. G. S. Bidwell. 1989. Mechanism of photosynthetic carbon dioxide uptake by the red macroalga, *Chondrus crispus*. Plant Physiol. 89:93–99.

Spalding, M. H. 1998. CO_2 acquisition: acclimation to changing carbon availability. Pp. 529–547. *in* J.-D. Rochaix, M. Goldschmidt-Clermont, and S. Merchant, eds. The molecular biology of chloroplasts and mitochondria in chlamydomonas. Kluwer Academic Publishers, Dordrecht, The Netherlands.

Stamatakis, A. 2006. RAxML-VI-HPC: maximum likelihood-based phylogenetic analyses with thousands of taxa and mixed models. Bioinformatics 22:2688–2690.

Suffrian, K., K. G. Schulz, M. A. Gutowska, U. Riebesell, and M. Bleich. 2011. Cellular pH measurements in *Emiliania huxleyi* reveal pronounced membrane proton permeability. New Phytol. 190:595–608.

Sun, S., F. Wang, C. Li, S. Qin, M. Zhou, L. Ding, et al. 2008. Emerging challenges: Massive green algae blooms in the Yellow Sea. Available at http://precedings.nature.com/documents/2266/version/1/files/npre20082266-1.pdf. (accessed 27 March 2014).

Takahashi, T., S. C. Sutherland, D. W. Chipman, J. G. Goddard, C. Ho, T. Newberger, et al. 2014. Climatological distributions of pH, pCO_2, total alkalinity, and $CaCO_3$ saturation in the global surface ocean, and temporal changes at selected locations. Mar. Chem. 164:95–125.

Thiers, B. 2014. Index Herbariorum: A global directory of public herbaria and associated staff. Available at http://sweetgum.nybg.org/ih/. (accessed 29 April 2014).

van de Waal, D. B., A. M. Verschoor, J. M. H. Verspagen, E. van Donk, and J. Huisman. 2010. Climate-driven changes in the ecological stoichiometry of aquatic ecosystems. Front. Ecol. Environ. 8:145–152.

Wang, Y., D. Dunamu, and M. H. Spalding. 2011. Carbon dioxide concentrating mechanism in *Chlamydomonas reinhardtii*: inorganic carbon transport and CO_2 recapture. Photosynthesis Res. 109:115–122.

Wilbur, K. M., and N. G. Anderson. 1948. Electrometric and colorimetric determination of carbonic anhydrase. J. Biol. Chem. 176:147–154.

Xu, J., and K. Gao. 2012. Future CO_2-induced ocean acidification mediates the physiological performance of a green tide alga. Plant Physiol. 160:1762–1769.

Xu, J. F., X. W. Zhang, N. H. Ye, Z. Zheng, S. L. Mou, M. T. Dong, et al. 2013. Activities of principal photosynthetic enzymes in green macroalga *Ulva linza*: functional implication of C-4 pathway in CO_2 assimilation. Sci. China Life Sci. 56:571–580.

Ye, R.-X., Z. Yu, W.-W. Shi, H.-J. Gao, Y.-H. Bi, and Z.-G. Zhou. 2014. Characterization of α-type carbonic anhydrase (CA) gene and subcellular localization of α-CA in the gametophytes of *Saccharina japonica*. J. Appl. Phycol. 26:881–890.

Young, E. B., M. Giordano, and J. Beardall. 2001. Investigation of inorganic carbon acquisition by *Dunaliella tertiolecta* (Chlorophyta) using inhibitors of putative HCO_3^- utilization pathways. Eur. J. Phycol. 36:81–88.

Zeebe, R. E., and D. Wolf-Gladrow. 2001. P. 360. CO_2 in seawater: equilibrium, kinetics, isotopes. Elsevier Oceanography Series, Amsterdam, The Netherlands.

Zhang, X., N. Ye, C. Liang, S. Mou, X. Fan, J. Xu, et al. 2012. De novo sequencing and analysis of the *Ulva linza* transcriptome to discover putative mechanisms associated with its successful colonization of coastal ecosystems. BMC Genom. 13:565.

Supporting Information

Additional Supporting Information may be found in the online version of this article:

Table S1. Identification of putative carbon concentrating mechanism (CCM) elements from *Ulva prolifera* expressed sequence tag (EST) libraries (Jia et al. 2011).